Supporting Information

Chiral recognition of optically active $CoFe_2O_4$ magnetic nanoparticles by chiral CdSe/CdS quantum dots

A.K. Visheratina,[*a] F. Purcell-Milton,[b] R. Serrano,[b] V.A. Kuznetsova[b], A.O. Orlova[a], A.V. Fedorov[a], A.V. Baranov[a] and Y.K. Gun'ko[*ab]

a. ITMO University, St. Petersburg, 197101, Russia.
E-mail: a.k.visheratina@gmail.com
b. School of Chemistry and CRANN, University of Dublin, Trinity College, Dublin 2, Ireland.
E-mail: igounko@tcd.ie

Graphical abstract

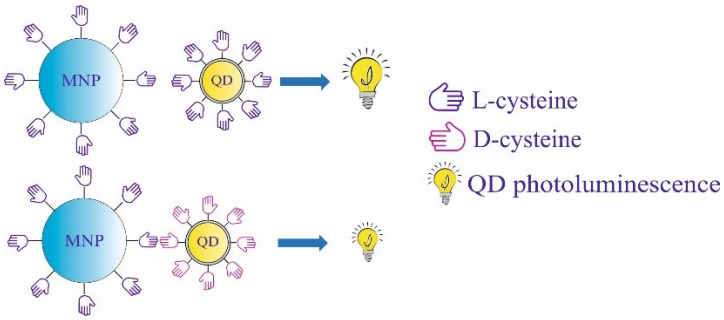

Cysteine stabilized $CoFe_2O_4$ magnetic nanoparticles

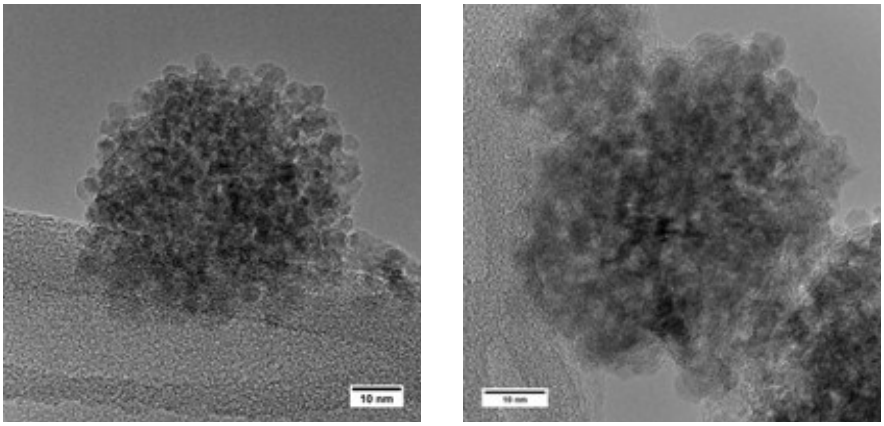

Fig. S1. TEM images of D-Cys stabilized $CoFe_2O_4$ MNPs.

FTIR spectrum of free cysteine (see Fig. S2) and cysteine stabilized MNPs (see Fig. S3) have the same characteristic bands except two strong bands observed at 545 cm^{-1} and 356 cm^{-1} in the MNP FTIR spectrum. These two vibrations bands, which can also be observed in FTIR spectrum of bare MNPs, correspond to the intrinsic lattice vibrations of octahedral and tetrahedral coordination compounds in the spinel structure, respectively. The presence of characteristic cysteine absorption bands in the MNP FTIR spectrum and the absence of the cysteine S-H peak at the same time indicate that cysteine attaches to MNP surface as thiolates.

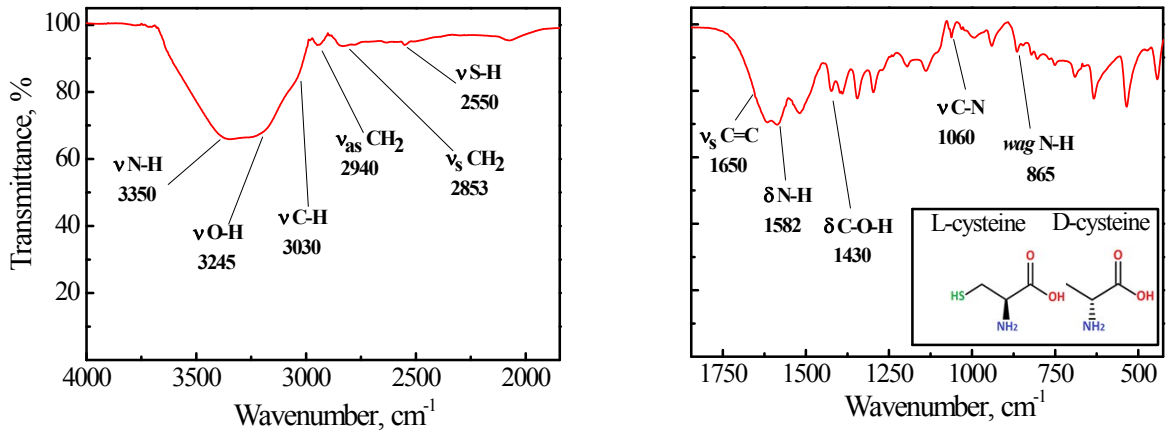

Fig. S2. FTIR spectra of cysteine molecules. The insert shows structural formula of both L- and D-cysteine molecules.

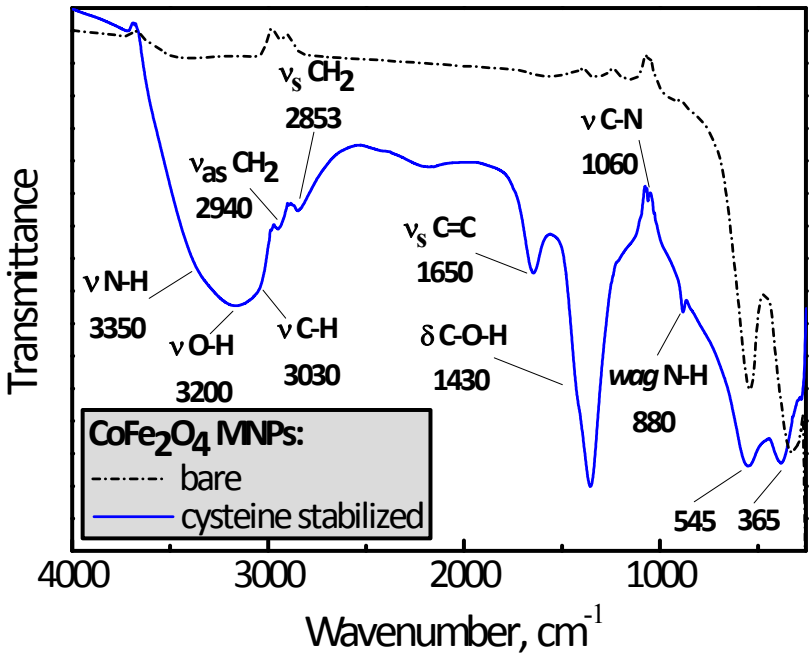

Fig. S3. FTIR spectra of bare and D-Cys stabilized $CoFe_2O_4$ MNPs.

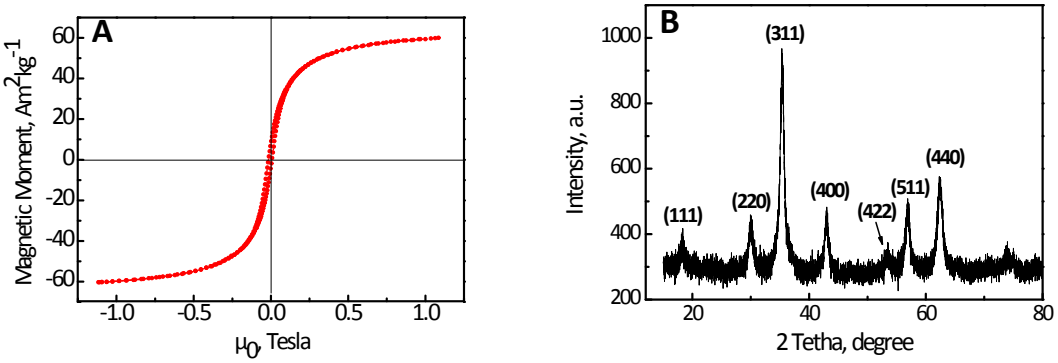

Fig. S4. (A) Magnetization curve; (B) XRD patterns of D-Cys stabilized $CoFe_2O_4$ MNPs.

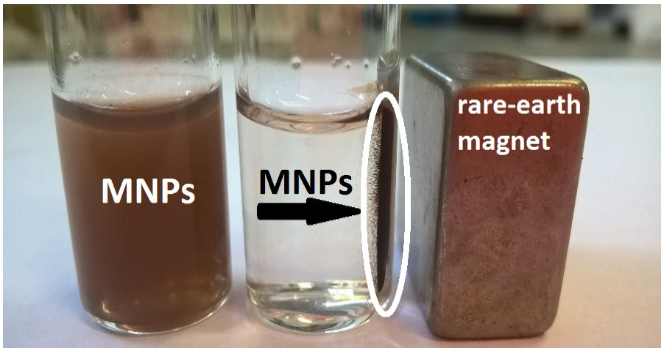

Fig. S5. MNP washing principle: after the MNP aqueous solution becomes transparent, the supernatant can be accurately removed, and MNPs can be resuspended in DMSO.

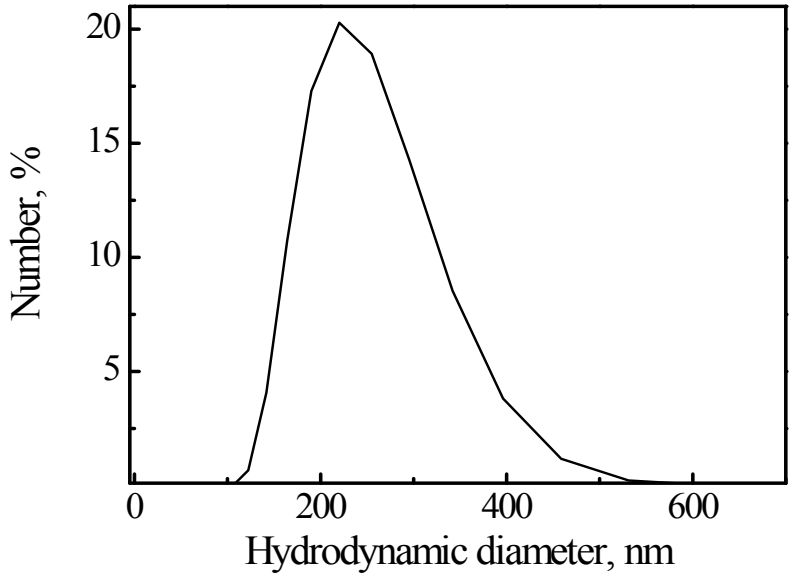

Fig. S6. DLS spectra of D-Cys stabilized $CoFe_2O_4$ MNPs in DMSO.

Cysteine stabilized CdSe/CdS quantum dots

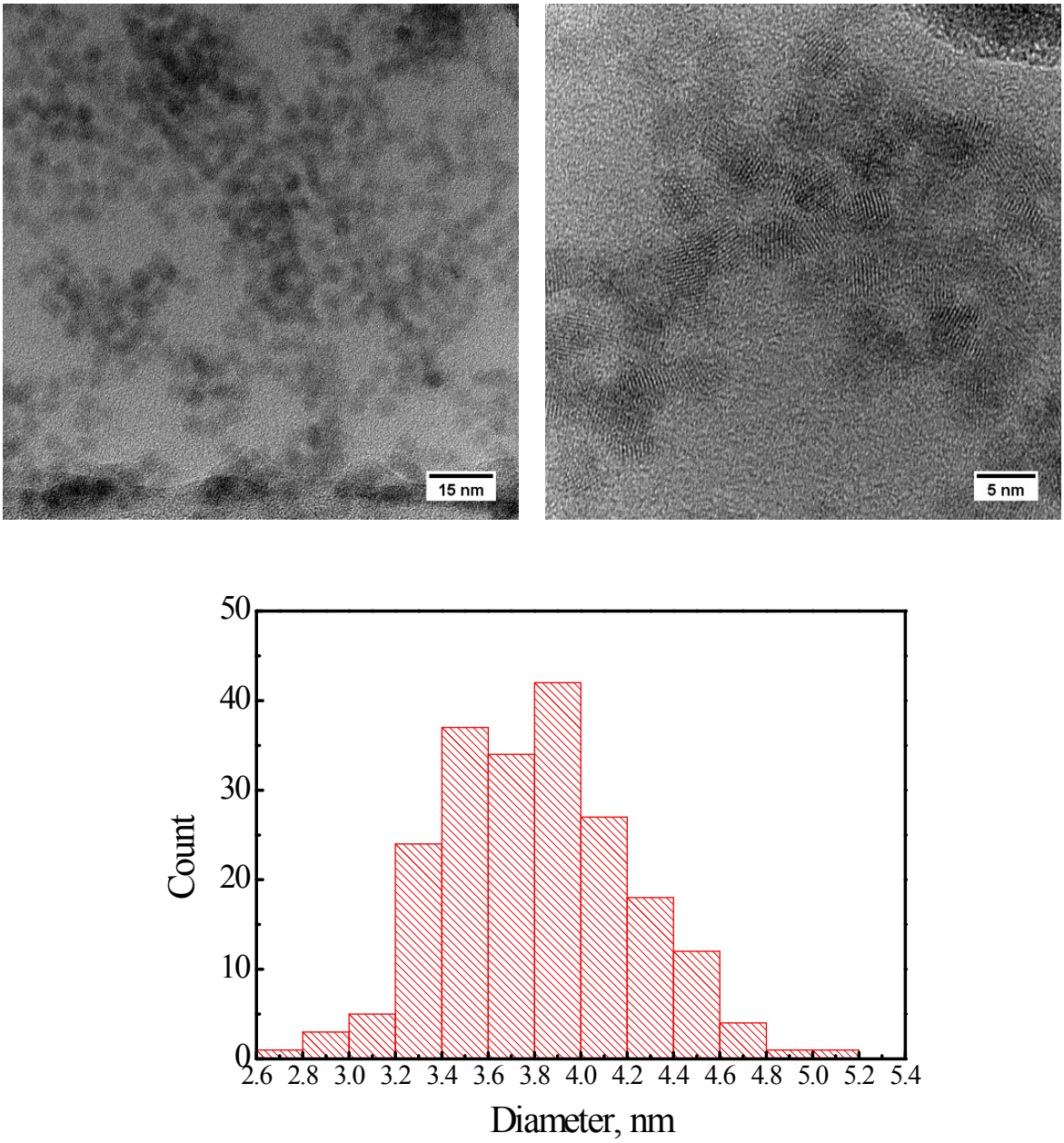

Fig. S7. TEM images and size distribution diagram of the CdSe/CdS QDs in heptane.

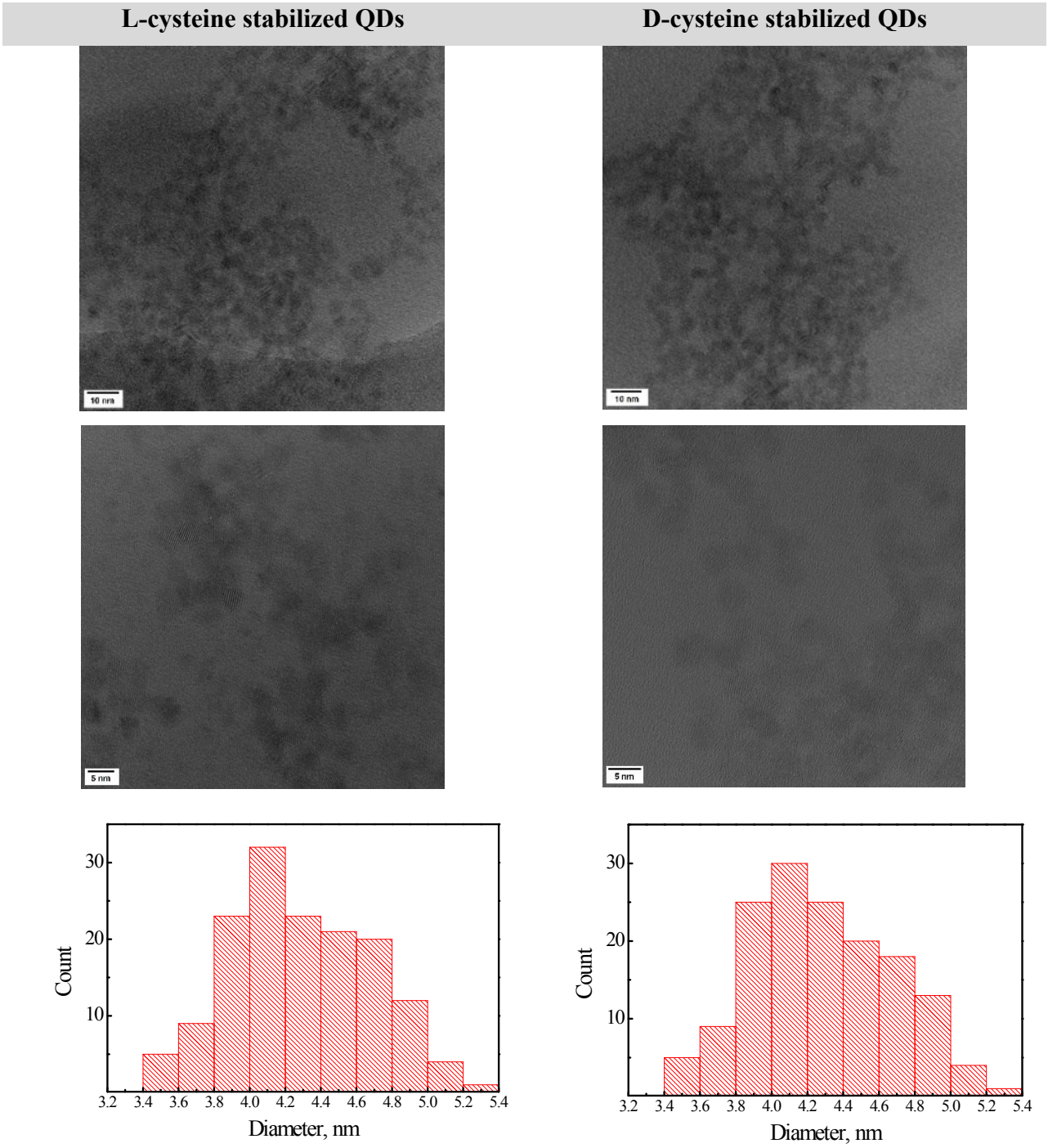

Fig. S8. TEM images and size distribution diagrams of the cysteine stabilized CdSe/CdS QDs in water.

As shown in Fig. S9, FTIR spectrum of oleylamine stabilized CdSe/CdS QDs shows clearly identified characteristic absorption bands from hydrocarbon groups: CH_3 asymmetric stretching vibration (ν_{as}=2955 cm^{-1}), CH_2 asymmetric (ν_{as}=2926 cm^{-1}) and symmetric (ν_s=2853 cm^{-1}) stretching vibrations, CH_2 bending vibration δ_s 1465 cm^{-1}), out-of-plane C-H bend (δ_s=915 cm^{-1}), and CH_2 rocking band (ρ=720 cm^{-1}). At the same time, the FTIR spectrum shows a N–H bending band (δ_s=1560 cm^{-1}), and C=C stretch at 1642 cm^{-1}. These indicate the presence of oleylamine on the QD surface.

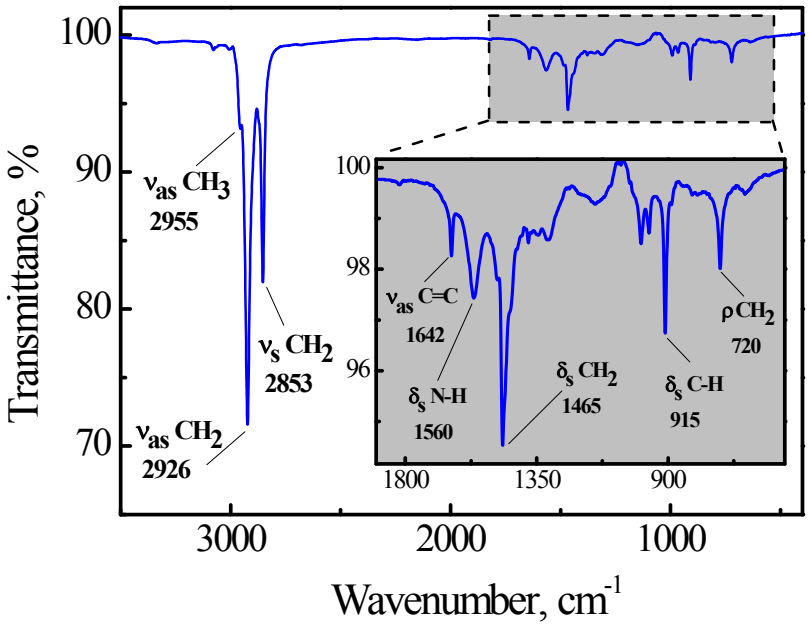

Fig. S9. FTIR spectrum of oleylamine stabilized CdSe/CdS QDs.

Fig. S10 represents FTIR spectra of free cysteine and cysteine stabilized CdSe/CdS QDs. In ligand FTIR spectrum, the intense band at 3245 cm^{-1} related to the broad intermolecular hydrogen bounded O-H stretch overlaps with secondary amine N-H stretching band at 3350 cm^{-1}. The following stretching vibrations from hydrocarbon groups can be also identified: C-H (ν=3030 cm^{-1}), CH_2 (ν_{as}=2940 cm^{-1}), CH_2 (ν_s=2853 cm^{-1}). The peak at 2550 cm^{-1} of cysteine molecules represents the δ(S–H) stretching vibration. Peaks at 1650 cm^{-1}, 1582 cm^{-1}, 1430 cm^{-1}, 1060 cm^{-1} and 865 cm^{-1} correspond to C=C stretching, N-H bending, C-O-H bending, C-N stretching and N-H wagging vibrations, respectively. The presence of characteristic cysteine absorption bands in the QD FTIR spectrum and the absence of the S-H peak (2550 cm−1) at the same time indicates, that the cysteine molecules chemisorbs as thiolates to the QD surface.

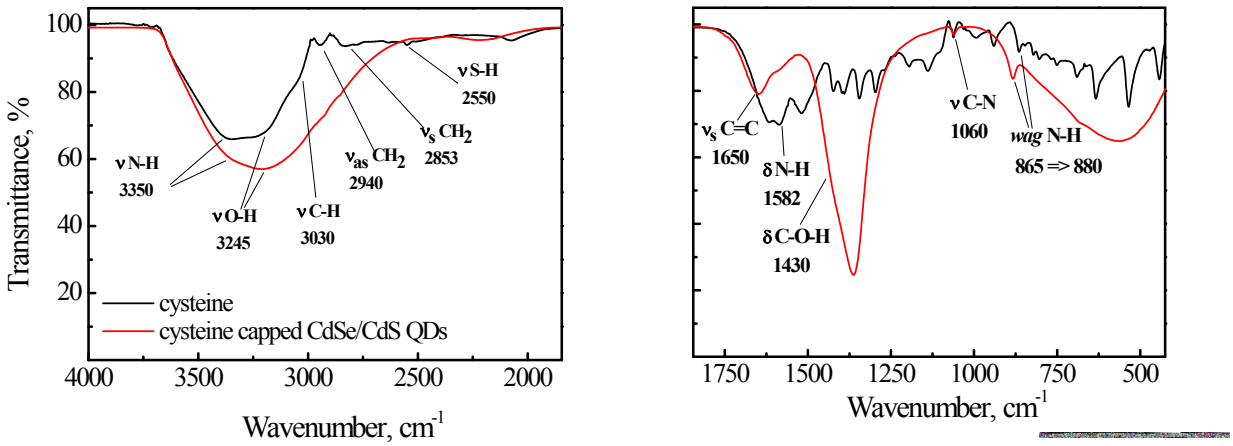

Fig. S10. FTIR spectra of free L-cysteine ligands and CdSe/CdS QDs stabilized with L-cysteine.

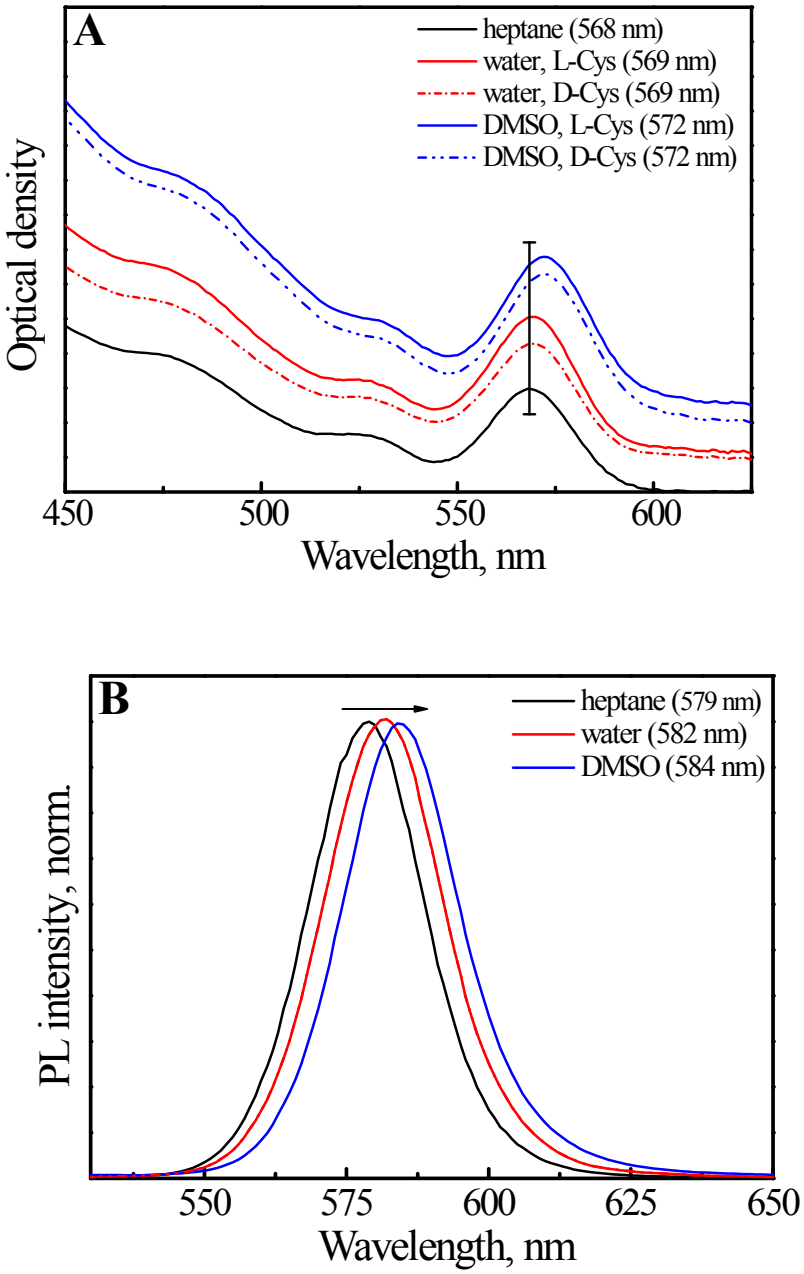

Fig. S11. Optical properties of CdSe/CdS QDs before and after phase transfer: (A) absorption and (B) PL spectra in different solvents. Numbers within brackets are wavelength of the QD first absorption band and PL maximum positions.

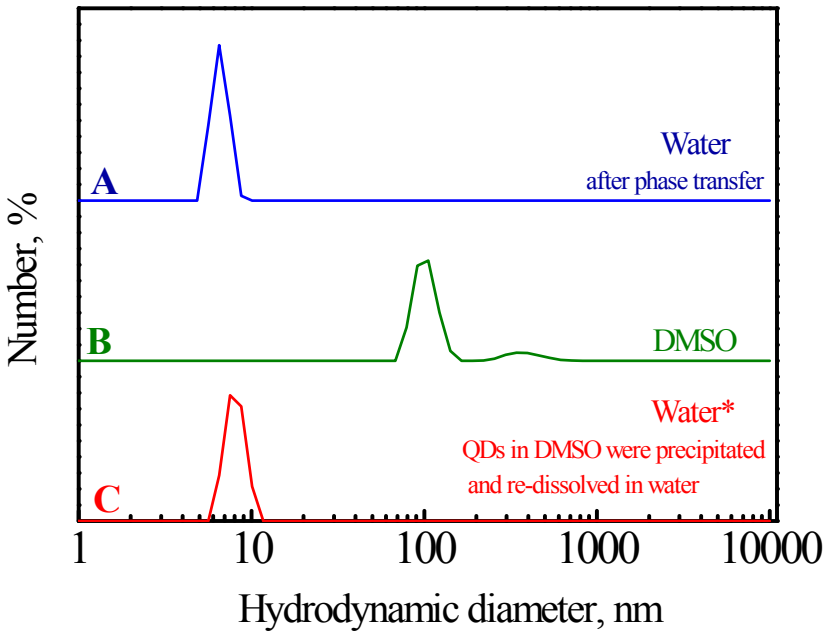

Fig. S12. DLS data on CdSe/CdS QDs in water and DMSO.

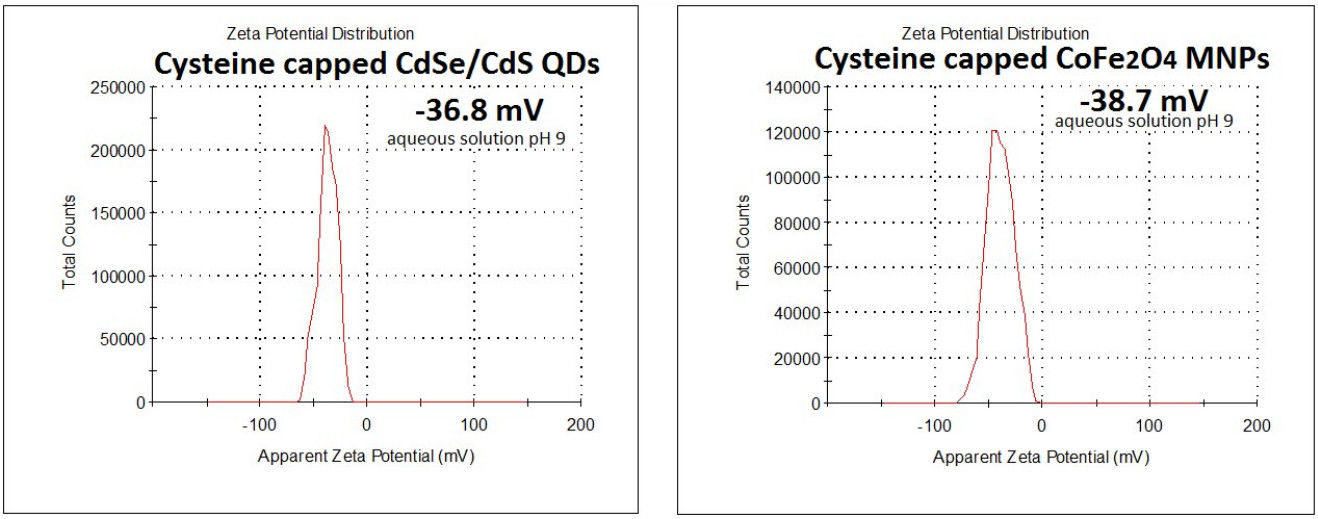

Fig. S13. Zeta potential distribution graphs of both cysteine capped CdSe/CdS QDs and $CoFe_2O_4$ MNPs in aqueous solution at pH 9.

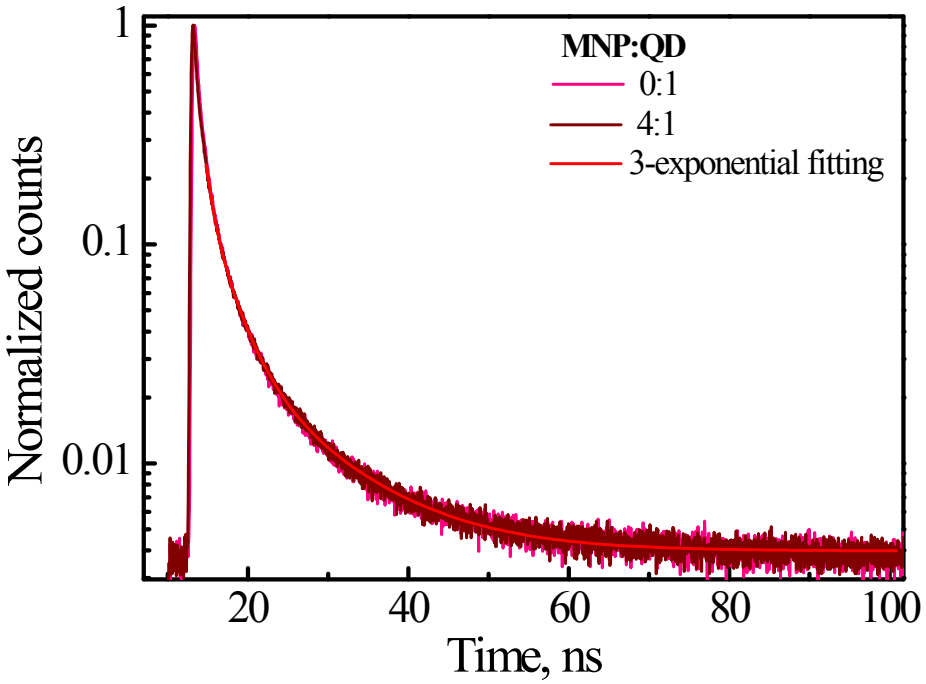

Fig. S14. PL decay curves for free QDs and for QDs in complexes with MNPs at C_{MNP}/C_{QD} ratio 4:1, where C is molar concentration.